Cortex Unfolding Using Level Set Methods

Gerardo Hermosillo, Olivier Faugeras, José Gomes

INRIA

INSTITUT NATIONAL DE RECHERCHE EN INFORMATIQUE ET EN AUTOMATIQUE

Cortex Unfolding Using Level Set Methods

Gerardo HERMOSILLO Olivier FAUGERAS and José GOMES

N° 3663

Avril 1999

THÈME 3

ISSN 0249-6399

Cortex Unfolding Using Level Set Methods

Gerardo HERMOSILLO Olivier FAUGERAS and José GOMES

Thème 3 — Interaction homme-machine,
images, données, connaissances
Projet Robotvis

Rapport de recherche n° 3663 — Avril 1999 — 16 pages

Abstract: We approach the problem of unfolding the surface of the cerebral cortex by modeling the problem as a front propagation governed by a Partial Differential Equation (PDE) which is solved using level set techniques. As a first step in this direction, we present multi-scale representations of closed surfaces that preserve their total area or enclosed volume. This is the three-dimensional extension of previous work on curves [21]. The resulting evolution equations allow the smoothing of closed surfaces without shrinkage. Additionally, correspondences between points in the surface at different scales are maintained by tracking the points of an initial mesh by means of an Ordinary Differential Equation (ODE). This technique allows to give tangential velocities to those points, therefore permitting them to move under general (tangential plus normal) velocity fields. We present the level set implementation of the normalized three-dimensional mean curvature flows and provide experimental results by unfolding surfaces segmented from MRI images of the human brain.

Key-words: *Front Propagation, Level Sets, Cortex unfolding, Mean Curvature Flow, Partial Differential Equations,*

Unité de recherche INRIA Sophia Antipolis
2004, route des Lucioles, B.P. 93, 06902 Sophia Antipolis Cedex (France)
Téléphone : 04 92 38 77 77 - International : +33 4 92 38 77 77 — Fax : 04 92 38 77 65 - International : +33 4 92 38 77 65

Gonflement du Cortex par des Méthodes de Surfaces de Niveau

Résumé : Nous modélisons le problème du gonflement du cortex cérébral comme un problème de propagation de front, régit par une Equation Différentielle Partielle que l'on résoud par des méthodes de surfaces de niveau. Dans cet article, nous présentons des représentations multi-échelles de surfaces fermées qui préservent l'aire totale ou le volume fermé. Ceci est une extension directe d'un travail antérieur pour des courbes planes [21]. Les équations d'évolution qui en résultent permettent le lissage de surfaces fermées sans rétrécissement. En outre, les correspondances entre points de la surface à des échelles différentes sont maintenues en suivant les points d'un maillage initial par une Equation Différentielle Ordinaire. Cette technique permet de donner des mouvements tangentiels à ces points, leur permettant ainsi de bouger sous l'action de champs de vitesse généraux (i.e. contenant des composantes tangentielles et normales). Nous présentons la mise en œuvre des équations proposées ainsi que les résultats expérimentaux en les appliquant sur des surfaces du cortex, segmentées à partir d'images IRM du cerveau humain.

Mots-clés : *Propagation de Fronts, Coupes de niveaux, Gonflement du Cortex, Flux par Courbure Moyenne, EDP*

Contents

1 Introduction

Neural activity in high-level tasks of the brain takes place mainly in the cortex, which in humans is a highly folded surface with more than half of its area hidden inside folds [23, 17, 24, 10]. Regions of neural activity which are close together in three-dimensional space may therefore be far apart when following the geodesic connecting them on the cortical surface. This suggests that a surface representation is better suited when doing functional analysis than a volumetric one [23, 24, 7].

Once such a representation is in hand, it may be necessary to "unfold" the surface in order to improve visualization and analysis of the neural activity. Presently, this is commonly done by representing the surface as a triangulated mesh which is forced to move depending on the gradient of a certain energy measure [7, 23].

This is a geometric Lagrangian formulation which can be exchanged for an Eulerian one, viewing the problem as a front propagation driven by a PDE. This so called "level set formulation" was initially proposed by Osher and Sethian [18] and has been extensively applied to curves [2, 8, 19, 15] and to a less extent to surfaces [12, 5, 3].

Although the Eulerian formulation has several advantages like the fact that it ensures that the evolving surface does not self-intersect and allows avoiding local minima where a Lagrangian formulation can not (see for example the discussion on min-max flow in [22]), at least two problems arise when migrating to a level set approach. The first one is that point correspondence between surfaces at different scales is not available. This problem was addressed in [1] where a method is suggested for tracking region boundaries. This solution however may not be sufficient since in general we wish to be able to map a function on the whole surface, e.g. neural activity. The second problem is due to the fact that the level set approach can only deal with flows that do not contain tangential velocities.

These two problems are in fact related. In the level set approach, only geometrical properties of the surface itself are accessible. The correspondence problem is that of maintaining the knowledge of a function defined on the surface but not related to its geometry. Tangential velocities are not possible precisely because they do not affect the geometry of the surface, although they *would* affect any extrinsic function defined on it.

We suggest that mapping the function of interest on the nodes of a mesh and subsequently tracking these nodes by means of an ODE may provide a solution to both problems simultaneously. The tracking of the mesh solves the correspondence problem and, at the same time, tangential velocities are applicable to those tracked nodes. In addition, topological changes may be handled automatically by re-sampling the function on the new triangulation extracted from the level set at each step. We therefore would have a hybrid approach in between the Eulerian and Lagrangian formulations in the form of an iterative three-step tracking algorithm:

1. Sample the function of interest on the nodes of a mesh extracted from the level-set, say by marching-cubes.

2. Compute one step of the evolution of this mesh according to the relevant PDE, possibly including tangential velocity terms (Lagrangian step).

3. Compute one step of the evolution of the level sets, reproject the tracked points on the zero level set (Eulerian step).

As a first attempt in experimenting with these ideas we present the three-dimensional extension of the flows presented in [21], representing Euclidean heat flows without shrinkage for closed surfaces. The obtained flows allow smoothing the surface while keeping the total area or enclosed volume constant. We give experimental results on the use of these flows to unfold the human cortex while tracking the initial triangulated representation as described above, but without remapping it during the evolution. The reason for not doing so is that in our particular application topological changes are not desirable. Maintaining the initial triangulation of the tracked nodes allows to identify more easily where those changes occur.

The remainder of the paper is organized as follows. In section 2, we present the evolution equations obtained by deforming the surface under mean curvature flow while simultaneously magnifying the space. Two cases are treated: constant volume and constant area. In section 3, we present the level set formulation of these flows. Section 4 discusses the proposed method to maintain the knowledge of a function defined on the surface during the evolution and experimental results are given in section 5. Finally, conclusions and future research directions are discussed in section 6.

2 Normalized 3D Mean Curvature Flows

In this section we will present the evolution equations for mean curvature flows with constant total area or enclosed volume. These are direct extensions of the Euclidean flows described by Sapiro and Tannenbaum [21] for planar curves. We will concentrate on the derivation of the evolution equations as also stated in [20]. In the sequel, bold letters will represent 3D vector quantities, the integral symbol will always denote a closed surface integral over the surface and the scalar and cross product between two vectors $v1$ and $v2$ will be denoted $v1 \cdot v2$ and $v1 \times v2$ respectively. Also, subscripts will denote partial differentiation with respect to the subscripted parameter.

We consider the family of surfaces in $\mathbb{R}^3$ denoted $\mathbf{S}(u, v, t)$, where u and v parameterize each surface and t parameterizes time (scale), which is obtained by the time evolution of an initial surface $\mathbf{S}_o(u, v) = \mathbf{S}(u, v, 0)$ governed by the following PDE:

$$\mathbf{S}_t = H\mathbf{N} \tag{1}$$

where $H(u, v)$ is the mean curvature and $\mathbf{N}(u, v)$ is the unit inward normal vector. This evolution is known as mean curvature flow and its properties have been extensively studied in the past [4, 13, 14, 16, 6].

The key idea to obtain a normalized flow is to apply a scaling to the space at each instant during the evolution. The scaling factor will be denoted $\psi(t)$. Let $\tilde{\mathbf{S}}$ be the image of $\mathbf{S}$ under this scaling:

$$\tilde{\mathbf{S}}(t) = \psi(t)\mathbf{S}(t) \tag{2}$$

Initially, $\psi(t) = 1$ and the two surfaces coincide. As time evolves, $\tilde{\mathbf{S}}$ describes another family of surfaces which adopts the same shapes as $\mathbf{S}$, since scaling is a similarity transformation. For the same reason, all the geometric properties of $\mathbf{S}$ can be inferred from those of $\tilde{\mathbf{S}}$. The function $\psi(t)$ can be chosen such that the volume of $\tilde{\mathbf{S}}$ remains constant:

$$\tilde{V} = \psi^3 V = V_0 \tag{3}$$

or such that the total area is preserved:

$$\tilde{A} = \psi^2 A = A_0 \tag{4}$$

The evolution of $\tilde{\mathbf{S}}$ with respect to t is given by:

$$\tilde{\mathbf{S}}_t = \psi_t \mathbf{S} + \psi \mathbf{S}_t = \psi_t \psi^{-1} \tilde{\mathbf{S}} + \psi^2 \tilde{H} \tilde{\mathbf{N}} \tag{5}$$

since we have $H = \psi \tilde{H}$ and $\mathbf{N} = \tilde{\mathbf{N}}$.

In order to normalize the second term in the right-hand side of (5) we perform a change of temporal variable, from t to $\tau(t)$:

$$\tilde{\mathbf{S}}_\tau = t_\tau \ (\psi_t \psi^{-1} \tilde{\mathbf{S}} + \psi^2 \tilde{H} \tilde{\mathbf{N}}) \tag{6}$$

We must then choose τ such that $t_\tau = \psi^{-2}$:

$$\tilde{\mathbf{S}}_\tau = \tilde{H} \tilde{\mathbf{N}} + \psi_t \psi^{-3} \tilde{\mathbf{S}} \tag{7}$$

Up to this point, we haven't specified ψ. The value of the term $\psi_t \psi^{-3}$ will depend on which quantity we wish to preserve. From (4) we obtain the area preserving value,

$$\psi_t \psi^{-3} = -\frac{1}{2} \frac{A_t}{A_0} \tag{8}$$

and from (3) we obtain the volume preserving one:

$$\psi_t \psi^{-3} = -\frac{1}{3} \frac{\psi V_t}{V_0} \tag{9}$$

We see that in order to achieve constant area or volume, we need to determine the evolutions of these quantities under mean curvature flow. As can be easily shown[1], the volume enclosed by the surface is given by

$$V = \frac{1}{3}\int \mathbf{S}\cdot\mathbf{N}\; d\sigma \tag{10}$$

while its total area is

$$A = \int d\sigma \tag{11}$$

To determine their evolutions, we first compute the evolutions of the area element

$$d\sigma = |\mathbf{S}_u \times \mathbf{S}_v|\; du\; dv \tag{12}$$

and that of the normal vector

$$\mathbf{N} = \frac{\mathbf{S}_u \times \mathbf{S}_v}{|\mathbf{S}_u \times \mathbf{S}_v|} \tag{13}$$

As is shown in the appendix, the evolution of the vector $\mathbf{S}_u \times \mathbf{S}_v$ can be decomposed into a normal and a tangential term as

$$(\mathbf{S}_u \times \mathbf{S}_v)_t = |\ \mathbf{S}_u \times \mathbf{S}_v\ |\ \ (2H^2\mathbf{N} - \nabla^t H) \tag{14}$$

Where $\nabla^t H$ is the tangent vector to the evolving surface giving the direction and the rate of maximum change of H, i.e. the projection of the gradient in the tangent plane of the evolving surface. From equation (14), the desired evolutions are readily obtained:

$$d\sigma_t = 2H^2 d\sigma \tag{15}$$

$$\mathbf{N}_t = -\nabla^t H \tag{16}$$

With these two equations in hand, the evolution of the area and enclosed volume follow immediately as the time derivatives of (11) and (10) respectively:

[1] The divergence theorem relates the volume integral of the divergence of a vector $\mathbf{A}$ to a surface integral over the surface bounding the volume as

$$\int_V \nabla\cdot\mathbf{A}\; dv = \int_S \mathbf{A}\cdot\mathbf{N}\; d\sigma$$

The fact that $\nabla\cdot\mathbf{S} = 3$ implies relation (10).

$$A_t = \int 2H^2 \, d\sigma \tag{17}$$

$$V_t = \frac{1}{3} \int (\, H - \mathbf{S} \cdot \nabla^t H + 2H^2 \, (\mathbf{S} \cdot \mathbf{N}) \,) \, d\sigma \tag{18}$$

Taking into account the relations $H = \psi \tilde{H}$, $\mathbf{S} = \psi^{-1} \tilde{\mathbf{S}}$, $\nabla^t H = \psi^2 \nabla^t \tilde{H}$ and $d\sigma = \psi^{-2} \tilde{d\sigma}$, these integrals may be computed on $\tilde{\mathbf{S}}$:

$$A_t = \int 2\tilde{H}^2 \, \tilde{d\sigma} \tag{19}$$

$$V_t = -\frac{1}{3\psi} \int (\tilde{H} + 2\tilde{H}^2 (\tilde{\mathbf{S}} \cdot \tilde{\mathbf{N}}) - \nabla^t \tilde{H} \cdot \tilde{\mathbf{S}}) \, \tilde{d\sigma} \tag{20}$$

allowing us to write the corresponding area and volume preserving flows by substitution in (7) of (8) and (9) respectively:

$$\tilde{\mathbf{S}}_\tau = \left(\tilde{H} + \frac{\tilde{\mathbf{S}} \cdot \tilde{\mathbf{N}}}{A_0} \int \tilde{H}^2 \, \tilde{d\sigma} \right) \tilde{\mathbf{N}} \tag{21}$$

$$\tilde{\mathbf{S}}_\tau = \left(\tilde{H} + \frac{\tilde{\mathbf{S}} \cdot \tilde{\mathbf{N}}}{9V_0} \int (\tilde{H} - \tilde{\mathbf{S}} \cdot \nabla \tilde{H} + 2\tilde{H}^2 (\tilde{\mathbf{S}} \cdot \tilde{\mathbf{N}})) \, \tilde{d\sigma} \right) \tilde{\mathbf{N}} \tag{22}$$

Note that the flows are geometrically intrinsic to $\tilde{\mathbf{S}}$. Also note that we have taken only the normal component of the second term in the equations, as only normal terms affect the geometry of the surface [21].

3 Level Set Formulation

We proceed to describe the computed flows under the level-set approach. A formal analysis may be found in [18, 11]. The surface is represented in an implicit form, as the zero level-set of a function $u(\mathbf{X}, t)$:

$$\mathbf{S}_o(u, v) \equiv \{\mathbf{X} \in \mathbb{R}^3 : u(\mathbf{X}, 0) = 0\} \tag{23}$$

If the surface is evolving according to

$$\frac{\partial \mathbf{S}}{\partial t} = \beta \mathbf{N} \tag{24}$$

then

$$\mathbf{S}(u,v,t) = \{\mathbf{X} \in \mathbb{R}^3 : u(\mathbf{X},t) = 0\} \qquad \forall t \tag{25}$$

provided that the function $u(\mathbf{X},t) : \mathbb{R}^3 \times \mathbb{R} \to \mathbb{R}$ deforms according to

$$\frac{\partial u}{\partial t} = \beta |\nabla u| \tag{26}$$

Intrinsic geometric properties of the surface have implicit expressions on u. For example the unit inward normal vector and the mean curvature are given by

$$\mathbf{N} = -\frac{\nabla u}{|\nabla u|} \tag{27}$$

and

$$H = \text{div}\frac{\nabla u}{|\nabla u|} \tag{28}$$

Actually the above values give the normal vector and mean curvature of the iso-level of u at $\mathbf{X}$. The only additional quantity that we require to implement the normalized flows is the tangential gradient of H. $\nabla^t H$ is obtained as the projection on the tangent plane of the gradient of the right-hand side of equation (28):

$$\nabla^t H = \nabla(\text{div}\frac{\nabla u}{|\nabla u|}) - \left(\nabla(\text{div}\frac{\nabla u}{|\nabla u|}) \cdot \frac{\nabla u}{|\nabla u|}\right)\frac{\nabla u}{|\nabla u|} \tag{29}$$

Finally, since the evolution equations are not local, the integrals must be approximated by extracting the corresponding integrands with a marching cubes technique.

4 Maintaining point correspondence at different scales

In this section we describe the tracking of the initial mesh of the surface, which contains information that is to be kept during the evolution. Formally, let

$$f(\mathbf{X}) : S \to \mathbb{R} \tag{30}$$

be a function on the surface, sampled at a finite number of points

$$\{\mathbf{X}_i \in S : f(\mathbf{X}_i) = f_i\} \tag{31}$$

Since the surface is evolving as $\mathbf{S}_t = \beta\mathbf{N}$, each of the points moves according to the following ODE:

$$\frac{d\mathbf{X}_i}{dt} = \beta(\mathbf{X}_i) \ \frac{\nabla u}{|\nabla u|}(\mathbf{X}_i) \qquad \forall i \tag{32}$$

Its trajectory can be followed by updating its position as

$$\mathbf{X}_i(t+\Delta t) \approx \mathbf{X}_i(t) + \beta \Delta t \, \frac{\nabla u}{|\nabla u|}(\mathbf{X}_i) \tag{33}$$

at each step of the PDE. Small systematic errors due to this approximation may be corrected at every iteration by projecting the points on the zero level set of u:

$$\mathbf{X}_i(t+\Delta t) \leftarrow \left(\mathbf{X}_i(t+\Delta t) - \frac{u}{|\nabla u|} \frac{\nabla u}{|\nabla u|}(\mathbf{X}_i(t+\Delta t)) \right) \tag{34}$$

Remapping the function on a new triangulation, for example to automatically account for changes in the surface topology, can be done in the following way. Let

$$Y = \{ \mathbf{Y}_j \in S : u(\mathbf{Y}_j) = 0 \} \tag{35}$$

be the set of nodes of the new mesh, which is extracted from u by a marching cubes technique. The function f can be remapped on Y by assigning to each $\mathbf{Y}_j$ the linear interpolation of f_k, f_l and f_m, where the three nodes $\mathbf{X}_k$, $\mathbf{X}_l$ and $\mathbf{X}_m$ are such that $\mathbf{Y}_j$ is inside the triangle of the tangent plane defined by the three points:

$$\left\{ \begin{array}{lllllll} \mathbf{P}_1 & = & \mathbf{X}_k & - & u\nabla u & / & |\nabla u|^2 \quad (\mathbf{X}_k) \\ \mathbf{P}_2 & = & \mathbf{X}_l & - & u\nabla u & / & |\nabla u|^2 \quad (\mathbf{X}_l) \\ \mathbf{P}_3 & = & \mathbf{X}_m & - & u\nabla u & / & |\nabla u|^2 \quad (\mathbf{X}_m) \end{array} \right. \tag{36}$$

To find such a triangle, a search is necessary among the closest triangles to $\mathbf{Y}_j$.

5 Results

Here we describe the results obtained by applying the normalized mean curvature flows together with the tracking framework described in the previous section, to unfold surfaces extracted from pre-segmented MRI images of the human brain. The tracked function in the examples is the sign of the mean curvature, light regions indicating concave folds.

Fig. 1 shows a first example starting with a reduced and slightly smoothed version of the cortex. This surface was obtained by applying a scaling flow:

$$\mathbf{S}_t = -(\mathbf{S} \cdot \mathbf{N})\mathbf{N} \tag{37}$$

to the cortex surface in order to reduce its size, followed by a few steps of Mean Curvature Flow (MCF). The columns correspond to three different views. The first row shows the initial surface. It can be observed that the relative areas of light and dark regions are approximately the same. This qualitative evaluation may already be useful in discarding flows that obviously change this balance.

This is the case for the constant area flow, whose results are shown in the second row of Fig. 1. It is clear that the dark regions become too wide while the light regions grow too thin. The relative areas of light and dark are not preserved at all. This is undesirable since the goal of the unfolding is to improve visibility in the light regions, i.e. the sulci. The third row is the result obtained with the constant volume flow. Here the proportion of dark and light regions is better preserved. The fourth row is the result obtained by applying MCF alone. The proportions are again qualitatively well preserved. Quantitative measures are required to evaluate more precisely these results.

The second example (Fig. 2) shows results with the original cortex surface extracted from the MRI image (i.e. no preprocessing was applied as in the previous example). In this case, only mean curvature flow and its constant volume version were tested. The first row shows the initial geometry of the cortex, while the second row presents the geometry as obtained by applying MCF with constant volume. In the third row, the sign-of-curvature function has been mapped on this same surface. The last row shows the result of applying MCF alone. The volume preserving flow appears to keep a better balance in light and dark regions than MCF alone.

6 Conclusion

We have presented normalized mean curvature flows together with a tracking framework that allows to maintain the knowledge of an extrinsic function defined on the surface. These flows were used as first attempts to solve the problem of unfolding the cortex using level set techniques, and have indeed yielded encouraging results. Nevertheless, further research is needed in order to obtain a front propagation model that takes into account the physical constraints of the problem, i.e. minimum variation of geodesic distances and no topological changes. By allowing tangential movements of the tracked nodes, our approach makes general propagation models (i.e. containing normal as well as tangential terms) applicable to those nodes.

Appendix

Here we show how to obtain equation (14), which gives the evolution of $\mathbf{S}_u \times \mathbf{S}_v$. Direct differentiation with respect to time gives:

$$(\mathbf{S}_u \times \mathbf{S}_v)_t = (H_u\mathbf{N} + H\mathbf{N}_u) \times \mathbf{S}_v + \mathbf{S}_u \times (H_v\mathbf{N} + H\mathbf{N}_v) \quad (38)$$

$$= \overbrace{\Big(H(\mathbf{N}_u \times \mathbf{S}_v + \mathbf{S}_u \times \mathbf{N}_v)\Big)}^{\mathcal{N}} - \overbrace{\Big(\ H_u\mathbf{S}_v \times \mathbf{N} + H_v\mathbf{N} \times \mathbf{S}_u\ \Big)}^{\mathcal{T}} \quad (39)$$

The first term is normal since $\mathbf{N}_u$, $\mathbf{N}_v$, $\mathbf{S}_u$ and $\mathbf{S}_v$ are all four tangential. Moreover, using the fact as stated in [9] that $\mathbf{N}_u$ and $\mathbf{N}_v$ are decomposed in the tangent plane as:

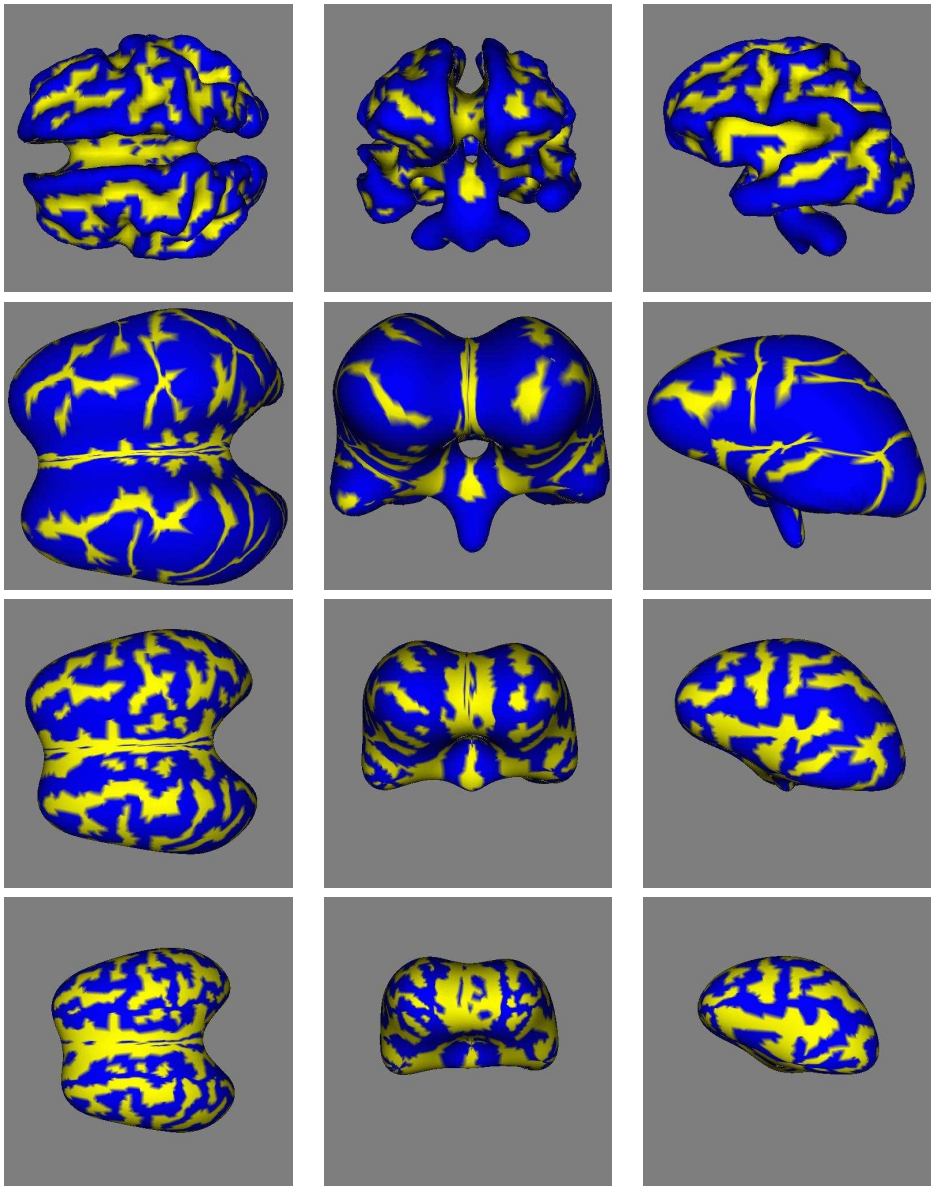

Figure 1: Results of cortex unfolding using the normalized flows. The columns represent three different views of the corresponding surface. From top to bottom: Original surface, MCF with constant area, MCF with constant volume, MCF alone. Note that due to the time normalization, the same number of steps corresponds to different stages of the shape evolution. Scale is the same in all three cases to make the amount of shrinkage evident. The starting surface is a reduced and smoothed version of the actual cortex.

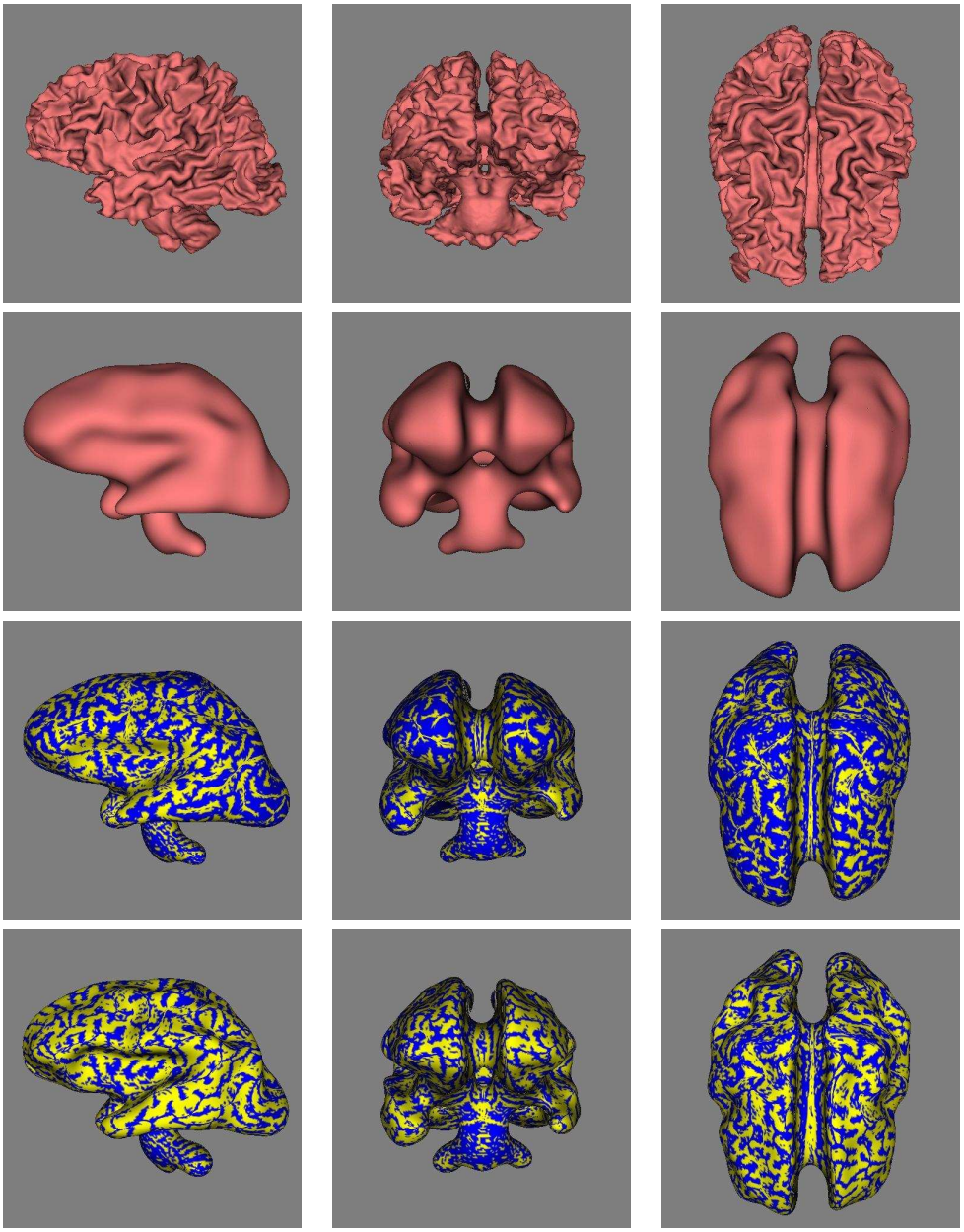

Figure 2: Unfolding the cortex as segmented from the MRI image. The first two rows show the geometry of the initial and final surfaces, without mapping the sign-of-curvature function. In the third row, the function is mapped using MCF with constant volume, while the fourth row shows the result of applying MCF alone.

$$\begin{aligned} \mathbf{N}_u &= a_{11}\mathbf{S}_u + a_{12}\mathbf{S}_v \\ \mathbf{N}_v &= a_{21}\mathbf{S}_u + a_{22}\mathbf{S}_v \end{aligned} \tag{40}$$

with

$$a_{11} + a_{22} = 2H \tag{41}$$

We have

$$\mathcal{N} = |\mathbf{S}_u \times \mathbf{S}_v| \, (2H^2\mathbf{N}) \tag{42}$$

The second term is obviously tangential and actually gives the gradient direction of H in the tangent plane. To see this, we will show that its scalar product with an arbitrary vector v of the tangent plane is proportional to the directional derivative of H in the direction of v, which is the definition of a gradient operator. Let v be expressed as

$$v = \alpha \, \mathbf{S}_u + \beta \, \mathbf{S}_v \tag{43}$$

We have

$$\mathcal{T} \cdot v = \alpha H_u \, \mathbf{S}_u \cdot (\mathbf{S}_v \times \mathbf{N}) + \beta H_v \, \mathbf{S}_v \cdot (\mathbf{N} \times \mathbf{S}_v) \tag{44}$$

but

$$\mathbf{S}_u \cdot (\mathbf{S}_v \times \mathbf{N}) = \mathbf{S}_v \cdot (\mathbf{N} \times \mathbf{S}_v) = |\mathbf{S}_u \times \mathbf{S}_v| \tag{45}$$

so that

$$\frac{1}{|\mathbf{S}_u \times \mathbf{S}_v|} \mathcal{T} \cdot v = \alpha H_u + \beta H_v \tag{46}$$

The right-hand side of equation (46) is the directional derivative of H in the direction of v. We therefore may write

$$\mathcal{T} = |\mathbf{S}_u \times \mathbf{S}_v| \, \nabla^t H \tag{47}$$

Combining equations (39), (42) and (47) gives equation (14):

$$(\mathbf{S}_u \times \mathbf{S}_v)_t = | \, \mathbf{S}_u \times \mathbf{S}_v \, | \;\; (2H^2\mathbf{N} - \nabla^t H) \tag{48}$$

References

[1] M. Bertalmio, G. Sapiro, and G. Randall. Region tracking on level-sets methods. *IEEE Transactions On Medical Imaging*, to appear.

[2] V. Caselles, R. Kimmel, and G. Sapiro. Geodesic active contours. In *Proceedings of the 5th International Conference on Computer Vision*, pages 694–699, Boston, MA, June 1995. IEEE Computer Society Press.

[3] V. Caselles, R. Kimmel, G. Sapiro, and C. Sbert. 3d active contours. In M-O. Berger, R. Deriche, I. Herlin, J. Jaffre, and J-M. Morel, editors, *Images,Wavelets and PDEs*, volume 219 of *Lecture Notes in Control and Information Sciences*, pages 43–49. Springer, June 1996.

[4] Y.G. Chen, Y. Giga, and S. Goto. Uniqueness and existence of viscosity solutions of generalized mean curvature flow equations. *J. Differential Geometry*, 33:749–786, 1991.

[5] David L. Chopp. Computing minimal surfaces via level set curvature flow. *Journal of Computational Physics*, 106:77–91, 1993.

[6] D.L. Chopp and J.A. Sethian. Flow under curvature: singularity formation, minimal surfaces, and geodesics. *Experimental Mathematics*, 2(4):235–255, 1993.

[7] Anders M. Dale and Martin I. Sereno. Improved localization of cortical activity by combining eeg and meg with mri cortical surface reconstruction: A linear approach. *Journal of Cognitive Neuroscience*, 5(2):162–176, 1993.

[8] Rachid Deriche, Stéphane Bouvin, and Olivier. Faugeras. Front propagation and level-set approach for geodesic active stereovision. In *Third Asian Conference On Computer Vision*, Bombay, India, January 1998.

[9] M. P. DoCarmo. *Differential Geometry of Curves and Surfaces*. Prentice-Hall, 1976.

[10] D. C. Van Essen, H.A. Drury, S.Joshi, and M.I. Miller. Functional and structural mapping of human cerebral cortex: Solutions are in the surfaces. In *Proceedings of the National Academy Science*, 1998.

[11] L.C. Evans and J. Spruck. Motion of level sets by mean curvature: I. *Journal of Differential Geometry*, 33:635–681, 1991.

[12] Olivier Faugeras and Renaud Keriven. Variational principles, surface evolution, pde's, level set methods and the stereo problem. *IEEE Trans. on Image Processing*, 7(3):336–344, March 1998.

[13] M. Gage and R.S. Hamilton. The heat equation shrinking convex plane curves. *J. of Differential Geometry*, 23:69–96, 1986.

[14] M. Grayson. The heat equation shrinks embedded plane curves to round points. *J. of Differential Geometry*, 26:285–314, 1987.

[15] R. Malladi, J. A. Sethian, and B.C. Vemuri. Shape modeling with front propagation: A level set approach. *PAMI*, 17(2):158–175, February 1995.

[16] R. Malladi and J.A. Sethian. Image processing: Flows under min/max curvature and mean curvature. *Graphical Models and Image Processing*, 58(2):127–141, March 1996.

[17] G. Orban. *Cerebral Cortex*, chapter 9, pages 359–434. Plenum Press, New York, 1997.

[18] S. Osher and J. Sethian. Fronts propagating with curvature dependent speed : algorithms based on the Hamilton-Jacobi formulation. *Journal of Computational Physics*, 79:12–49, 1988.

[19] N. Paragios and R. Deriche. A PDE-based Level Set Approach for Detection and Tracking of Moving Objects. In *Proceedings of the 6th International Conference on Computer Vision*, Bombay,India, January 1998. IEEE Computer Society Press.

[20] Alfons H. Salden. *Dynamic Scale Space Paradigms*. PhD thesis, Utrecht University, Medical Faculty, Heidelberglaan 100, Utrecht, The Netherlands, November 1996.

[21] G. Sapiro and A. Tannenbaum. Area and length preserving geometric invariant scale-spaces. *PAMI*, 17(1):67–72, January 1995.

[22] J. A. Sethian. *Level Set Methods*. Cambridge University Press, 1996.

[23] R. B. H. Tootell, J. D. Mendola, N. K. Hadjikhani, P. J. Leden, A. K. Liu, J. B. Reppas, M. I. Sereno, and A. M. Dale. Functional analysis of v3a and related areas in human visual cortex. *The Journal of Neuroscience*, 17(18):7060–7078, September 1997.

[24] K. Zilles, E. Armstrong, A. Schleicher, and H.-J.Kretschmann. *The Human Pattern of Gyrification in the Cerebral Cortex*, pages 173–179. 1988.

Unité de recherche INRIA Sophia Antipolis
2004, route des Lucioles - B.P. 93 - 06902 Sophia Antipolis Cedex (France)

Unité de recherche INRIA Lorraine : Technopôle de Nancy-Brabois - Campus scientifi que
615, rue du Jardin Botanique - B.P. 101 - 54602 Villers lès Nancy Cedex (France)
Unité de recherche INRIA Rennes : IRISA, Campus universitaire de Beaulieu - 35042 Rennes Cedex (France)
Unité de recherche INRIA Rhône-Alpes : 655, avenue de l'Europe - 38330 Montbonnot St Martin (France)
Unité de recherche INRIA Rocquencourt : Domaine de Voluceau - Rocquencourt - B.P. 105 - 78153 Le Chesnay Cedex (France)

Éditeur
INRIA - Domaine de Voluceau - Rocquencourt, B.P. 105 - 78153 Le Chesnay Cedex (France)
http://www.inria.fr
ISSN 0249-6399